Performance analysis of a point-absorber wave energy converter with a single buoy composed of three rigidly coupled structures

Aldo Ruezga, José M. Cañedo C., Manuel G. Verduzco-Zapata and Francisco J. Ocampo-Torres

Abstract — **A single-body point absorber system is analysed to improve its power absorption at a finite water depth. The proposed wave energy converter consists of a single floating body coupled to a direct-drive power take-off system placed on the seabed. The structure of a cylindrical buoy with large draft is changed by a single body composed of three structures rigidly coupled, reducing its volume and improving its frequency-dependent hydrostatic parameters that are obtained through a numerical analysis tool called NEMOH. The undamped natural frequency of the oscillating system is tuned to a specified wave period and the performance of the WEC system is obtained assuming a linear Power Take-Off system. In time domain, the performance of the WEC device is carried-out under a regular (sinusoidal) and irregular incident wave profile. Comparing the performance of the WEC system using the cylindrical and the proposed buoy outcomes that the system with the proposed buoy is able to absorb more energy from incident waves with a wider frequency range, whereas the oscillating system is kept as simple as possible.**

Keywords— **Point-absorber, Renewable energy, Wave energy.**

Manuscript received 19 August, 2020; revised 8 May, 2021; accepted 1 July, 2021; published 2 July, 2021.

A. Ruezga is at CINVESTAV, Zapopan, Jalisco, México (email: aruezga@gdl.cinvestav.mx)

J. M. Cañedo C. is with the Department of Electric Power Systems, CINVESTAV, Zapopan, Jalisco, México (email: jose.canedo@cinvestav.mx)

M. G. Verduzco-Zapata is at University of Colima (UCOL), Colima, Colima, México (email: manuel_verduzco@ucol.mx)

F. J. Ocampo-Torres is with Department of Physical Oceanography, CICESE, Ensenada, Baja California, México (email: ocampo@cicese.mx)

One of the authors was supported by *Consejo Nacional de Ciencia y Tecnologia* (CONACYT), México. Digital Object Identifier https://doi.org/10.36688/imej.4.37-45

NOMENCLATURE

Symbol	Description
F_i	Inertial force
F_h	Hydrostatic force
F_r	Radiation force
F_e	Excitation force
F_u	External force
F_k	Restrictive force
m_b	Buoy mass
$m_3(\omega)$	Added mass
m_∞	Added mass at infinite frequency
$B_3(\omega)$	Radiation damping
B_u	External damping coefficient
$f_e(\omega)$	Excitation force coefficient
η	Water surface elevation
S_b	Buoyancy stiffness
k_l	Restoring coefficient
A_{wp}	Water plane area
ρ	Water density
g	Gravity acceleration
r_b	Buoy radius
z	Buoy motion in heave
$\dot{z}$	Buoy velocity in heave
P_a	Useful power (average power)
ℓ	Capture width
λ	Wavelength
h_r	IRF of the radiation force
h_e	IRF of the excitation force
x_f	State spaces (excitation force)
x_r	State spaces (radiation force)

Abbreviation	Description
WEC	Wave energy Converter
PTO	Power Take-Off
RAO	Response Amplitude Operator
IRF	Impulse Response function
MB	Modified buoy
CB	Cylindrical buoy

I. INTRODUCTION

FROM the diverse renewable sources of energy, ocean waves contain a higher energy density than others, representing a large energy source with less intermittency [01].

Among the different types of devices categorized by the European Marine Energy Centre (EMEC), point absorber and submerged pressure-differential devices are capable of extracting wave energy from incoming waves in all directions. However, for a given sea state, both devices have different performance (e.g. if the wave

amplitude and period are low, it is preferable to use point-absorber devices [02]).

Point absorbers are axisymmetric devices of small dimensions in comparison to the incident wavelength (λ), typically characterized by a narrow frequency bandwidth, and generally, their natural frequency does not correspond with the frequency of dominant ocean waves [03] [04] [05] [06].

When the natural frequency of oscillation coincides with the frequency of the incident wave, the oscillating system has an optimal phase condition, the WEC enters in resonance with the excitation source, and the maximum transfer of wave energy to the system is obtained.

The optimal phase condition can be obtained through continuous and discrete control methods. A continuous phase control or reactive power control, requires that the power flow of the Power Take-off (PTO) system be reversed during some intervals of the Wave Energy Converter (WEC) oscillating cycle; thus, the PTO system must be able to supply energy to the oscillating system [03] [05] [06] [07]. This can be avoided if discrete control techniques are used; being the latching control the most common one. However, it is necessary that the device is equipped with clamping mechanisms or hydraulic valves depending on the PTO system used in order to retain the buoy position. The buoy is held at its maximum excursion when the buoy velocity drops to zero and it is released after a certain interval of time such that its velocity is in phase with the exciting force. One drawback of this technique is that latching control requires the prediction of incident waves [05] [06] [07] [08].

In addition to control schemes, the geometry and weight of the floating body in a Point-absorber WEC system have an influence on the device performance. Thus, an appropriate buoy dimensions leads to the natural frequency of the oscillatory system being shifted towards the frequency range of the dominant incident wave; improving the hydrodynamic performance of the WEC system and decreasing the control requirements. For this reason, several studies have focused on analyzing various sizes and shapes of floating bodies, with cylindrical, spherical, conical, and hemispherical forms being among the most common ones.

For a single-body point absorber device with a direct-drive PTO system equipped with a cylindrical buoy, several researchers have analyzed the influence of the buoy size (radius and draft) on the WEC performance. Eriksson et al. [09] analyzed the influence of the buoy radius on the WEC performance, maintaining the draft as a constant value. As a result, they indicate that the device capture ratio can be improved if the buoy radius is sufficiently large and the damping of the PTO system is controlled. However, as the draft is increased, the added mass increases whereas both excitation force and radiation damping decrease [10] [11]. Thus, the frequency bandwidth of the device is decreased and its natural frequency is shifted towards lower frequencies. Usha [12] analyzed the hydrodynamic performance of a cylindrical buoy and compared it with that of a spherical and a lenticular buoy, his results shows that the cylindrical buoy (rectangular cross section) provides a better power absorption. Other geometries were compared in [13] [14] [15] [16] and [17], where a better overall performance was obtained with a cylindrical buoy with conical bottom. However, to improve the hydrodynamic performance in a certain frequency range, the best option is a cylindrical buoy [12] [15].

Depending on the PTO and the structural characteristics of the device, some WEC are equipped with additional mechanical elements that allow them to adjust the natural frequency of the oscillating system. Some of them are analysed in [16] [17] [18] [19] and [20], where the natural frequency of the oscillating systems is tuned to the frequency of incident waves. However, the use of additional mechanisms could increase the cost and maintenance requirements of the WECs.

In a two-body point-absorber devices, a floating body reacts to a submerged body used as a point of reference and the PTO use the relative motion between both bodies to convert the wave energy [03]. Because the submerged body has a larger wet surface than the buoy at sea surface, it has a higher added mass and a lower radiation damping [21] [22], therefore, the submerged body remains at a relatively stationary position with respect to the floating body at sea surface. Blanco et al. [23] dimensioned and analyzed a two-body WEC system equipped with a direct-drive PTO to enhance its power absorption at deep water, resulting in large values of the dimensions for both bodies.

Based on characteristics of two-body systems, the Uppsala University adapted a single-body point absorber WEC to operate using two floating bodies, placing an intermediate body between the primary floating body and the PTO sited on the seabed [24] [25]. The second body adds inertia to the oscillating system and shifts its natural frequency towards dominant incident waves; therefore, the performance and the capture width ratio of the WEC device are increased. However, both bodies have to be placed at adequate distance to avoid a hydrodynamic interference between them, requiring deeper water conditions for deployment.

In this paper, a single-body point-absorber WEC with a direct-drive power take-off system placed at seabed is considered. Considering this configuration, the deployment site should have a micro-tidal regime in order to prevent the system from having extra stresses due to high water level changes. Furthermore, in deeper waters, the installation and recovery manoeuvres would be complicated.

Commonly, in this type of WEC, a large buoy is used to

shift the natural frequency of the WEC device towards the dominant incident wave frequencies. However, a buoy with large draft provides a narrow frequency bandwidth. Therefore, the geometry of a cylindrical buoy with large draft is modified by changing some parts of the structure, reducing its volume and increasing the buoy wet surface to enhance its frequency dependent hydrostatic parameters at a given water depth, improving the performance of the oscillating system and maximizing its power absorption capability.

Unlike two-body devices, where the secondary object provides a large added mass and low radiation damping, the submerged part in the composed-structure single-buoy is used to increase the added mass whereas the amplitude of the radiation damping is maintained as high as possible. The proposed buoy structure acts as a single floating body without relative motion between its structural parts and, despite the fact that it has a large draft; it also has a low volume and weight compared to an equivalent cylindrical buoy, and providing a better absorption wave power.

It is known that both the bathymetry and the wave energy resource at a given site influence the design of the WEC device. Therefore, if the WEC device is placed at a site with different characteristic, the WEC system will not provide the same performance. In most studies related to wave energy converters, sea states characterized by high-amplitude and long-period waves are usually taken into account. However, in this paper, a single-body point-absorber WEC is designed to operate in Mexican coastal waters in the Pacific Ocean, where the sea states are characterized by short-period waves and the wave energy resource is low to moderate in comparison to other places especially at higher latitudes.

II. DYNAMICS OF THE WAVE ENERGY CONVERTER

The linear wave theory is considered to model the behaviour of a WEC device. This theory assumes that the free-surface displacement (η) of the ocean water is much smaller than the wavelength (λ) of incident waves, and that the wavelength is greater than the radius (r_b) of the buoy. For a WEC device restricted to moving in one degree of freedom, motion in heave (z-axis), the dynamic equation of the oscillating system is obtained from Newton's second law of motion.

$$F_i = F_h + F_r + F_e + F_u + F_k \tag{1}$$

where $F_i = -m_b \omega^2 Z$ is the inertial force that is proportional to the buoy mass (m_b) multiplied by the buoy acceleration ($-\omega^2 Z$), and the terms on the right side are related to the forces that act on the floating body, corresponding to the hydrostatic force, radiation force, excitation force, an external force and a mechanical restrictive force, respectively. In addition, energy losses (viscous and friction forces) on the oscillating system are neglected, the foregoing considering that in a heavily damped system, the viscous damping is substantially less significant than external damping [25].

The radiation force is an induced force that acts on the buoy due to its own motion and does not depend on incident waves [26] [27] [28]. This force is defined by two frequency-dependent hydrostatic parameters named as radiation damping (B_3) and added mass (m_3). The radiation damping tends to zero as the frequency approaches infinity or zero, whereas the added mass is finite in both limits, and the radiation force can be described as

$$F_r = -\left[B_3(\omega) + i\omega m_3(\omega)\right]U \tag{2}$$

where ($U = i\omega Z$) is the floating body velocity. Unlike the radiation force, the excitation force acts on the buoy due to incident waves and it does not depend on the buoy motion. This force is defined by an excitation force coefficient ($f_e(\omega)$) that multiplies the water surface elevation (η) of the incident wave, such that

$$F_e = f_e(\omega)\eta \tag{3}$$

The hydrostatic force (F_h) is a hydrostatic restoring force that is proportional to the excursion of the buoy multiplied by a buoyancy stiffness (S_b), composed of the water plane area (A_{wp}) of the buoy, water density (ρ) and the acceleration of gravity (g):

$$F_h = -S_b Z = -\rho g A_{wp} Z \tag{4}$$

The external force represents the reaction force of the PTO system on the oscillating system, it is represented as a linear damping coefficient multiplied by the velocity (U) of the oscillating system as

$$F_u = -B_u U \tag{5}$$

The mechanical restrictive force (F_k) is included to represent mechanic restrictive elements on the oscillating system. This force is proportional to the buoy displacement in heave multiplied by a restoring coefficient (k_l).

$$F_k = -k_l Z \tag{6}$$

Replacing the force terms (2-6) in (1) and rearranging the equation gives the expression for the Response Amplitude Operator (RAO). The RAO is a dimensionless transfer function that describes the vertical displacement of the buoy within a frequency range related to incident waves, and it can be described as

$$\frac{Z}{\eta} = \frac{f_e(\omega)}{-\omega^2\left[m_b + m_3(\omega)\right] + i\omega\left[B_u + B_3(\omega)\right] + \left(S_b + k_l\right)} \tag{7}$$

The PTO damping (B_u) has an important role on the device performance, and in conjunction with the hydrostatic parameters of the oscillating system; it determines the useful power (average power) that the WEC system can obtain from the incident waves [10] [28], and is expressed as

$$P_a = 0.5\ \omega^2\ B_u\ \left|Z\right|^2 = 0.5 B_u \left|U\right|^2 \tag{8}$$

The length that an axisymmetric body must have to absorb the maximum theoretical power from incident waves is termed as capture width (ℓ), and it can be considered as an equivalent crest width equal to the wavelength (λ) divided by 2π [26] [28]

$$\mathrm{l} = P_{max}/\mathrm{J} = \lambda/2\pi \tag{9}$$

where P_{max} is the maximum absorbed power and J is the energy transported by incident waves. In time domain, the mathematical model of the WEC device dynamics is described by the Cummins integro-differential equation [29], such that

$$\begin{aligned}[m_b + m_3(\infty)]\ddot{z}(t) = &-h_r(t) * \dot{z}(t) - B_u\dot{z}(t) \\ &-(S_b + k_l)z(t) + h_e(t) * \eta(t)\end{aligned} \tag{10}$$

Where the terms related to radiation damping and excitation force are expressed by convolution terms. The convolution terms are related to an Impulse Response Function (IRF) of the radiation force (h_r) and the excitation force (h_e). The radiation IRF is a real-causal function ($h_r = 0$ for $t < 0$) and it can be obtained with the radiation damping [28] [30], whereas the excitation IRF is a non-causal function ($h_e \neq 0$ for $t < 0$) and it can be obtained applying the inverse Fourier transform to the excitation force coefficient [30] [32]. Therefore the expressions for the radiation and excitation forces are as follow

$$h_r = \left(2/\pi\right)\int_0^\infty B_3\left(\omega\right)\cos\left(\omega t\right)d\omega \tag{11}$$

$$h_e = \left(1/2\pi\right)\int_{-\infty}^{\infty} f_e\left(\omega\right)\exp\left(i\omega t\right)d\omega \tag{12}$$

As proposed by Yu and Falnes in [30] and [31], the convolution integrals are approximated by a state space representation of a linear subsystem, where its output corresponds to the solution of the approximate convolution operation, such that

$$\begin{aligned}\dot{\mathrm{X}}(t) &= \mathrm{A}\mathrm{X}(t) + \mathrm{B}u(t) \\ y(t) &= \mathrm{C}\mathrm{X}(t) \approx \textstyle\int_{-\infty}^{t} h_O(t-\tau)\,\dot{z}(\tau)d\tau\end{aligned} \tag{13}$$

where the input signal (u) in the state space model related to the radiation and excitation subsystem corresponds to the oscillation velocity ($\dot{z}$) of the buoy and the water surface elevation (η) of the incident wave, respectively. The state matrices $\boldsymbol{A}$, $\boldsymbol{B}$ and $\boldsymbol{C}$ have a companion-form realization, such that

$$\mathrm{A} = \begin{bmatrix} 0 & \cdots & \cdots & 0 & -a_1 \\ 1 & \ddots & & \vdots & -a_2 \\ 0 & 1 & \ddots & \vdots & \vdots \\ \vdots & \ddots & \ddots & 0 & -a_{n-1} \\ 0 & \cdots & 0 & 1 & -a_n \end{bmatrix} \quad \mathrm{B} = \begin{bmatrix} b_1 \\ b_2 \\ \vdots \\ b_{n-1} \\ b_n \end{bmatrix} \quad \mathrm{C} = \begin{bmatrix} 0 \\ \vdots \\ 1 \end{bmatrix}^T \tag{14}$$

The unknown coefficients of the state matrices in (13) are determined by minimizing the target function (Q) used in [30] [31]. This target function approximates the impulse response function of the state space model based on the impulse response function of radiation (h_r) and excitation (h_e), respectively, and it is expressed as

$$Q = \sum_{k=1}^{m} G\left(t_k\right)\left[h_O\left(t_k\right) - \mathbf{C}\exp\left(\mathbf{A}t\right)\mathbf{B}\right]^2 \tag{15}$$

where h_o is the IRF of the subsystem (radiation or excitation) that is used to characterize the state matrices. The weight function (G) can be a constant value greater than zero [31]. In the excitation subsystem, the non-causal impulse response function is causalized using a time shift (t_c) such that h_e is negligible for $t < -t_c$ and $t_c > 0$. The corresponding causalized impulse response function is $h_c = h_e(t - t_c)$ and therefore, the output (y_c) of the excitation subsystem at time (t) is influenced by the input at a future time [30], such that

$$y_c\left(t\right) = \mathbf{C}\,\mathbf{X}\left(t + t_c\right) \approx \textstyle\int_{-\infty}^{\infty} h_e\left(t - t_c - \tau\right)\eta\left(\tau\right)d\tau \tag{16}$$

Grouping (10) with (13) for both subsystems, radiation and excitation, the state space model of the WEC system has the form

$$\begin{bmatrix} \dot{x}_{f_1} \\ \vdots \\ \dot{x}_{f_n} \\ \dot{x}_{r_1} \\ \vdots \\ \dot{x}_{r_n} \\ \dot{z} \\ \ddot{z} \end{bmatrix} = \begin{bmatrix} & A_f & & 0 & \cdots & 0 & \\ & & & & & b_{r_1} & \\ & 0 & & A_r & \vdots & \vdots & \\ & & & & & b_{r_n} & \\ & 0 & & \cdots & 0 & 1 & \\ 0 & \cdots & c_1 & 0 & \cdots & -c_1 & -c_2 & -c_3 \end{bmatrix} \begin{bmatrix} x_{f_1} \\ \vdots \\ x_{f_n} \\ x_{r_1} \\ \vdots \\ x_{r_n} \\ z \\ \dot{z} \end{bmatrix} + \begin{bmatrix} b_{f_1} \\ \vdots \\ b_{f_n} \\ 0 \\ \vdots \\ 0 \end{bmatrix} \eta(t) \tag{17}$$

$$c_1 = \frac{1}{m_b + m_3(\infty)} \quad c_2 = \frac{S_b + k_l}{m_b + m_3(\infty)} \quad c_3 = \frac{B_u}{m_b + m_3(\infty)}$$

In the previous expressions, the state spaces correspond to the excitation force (x_f), radiation force (x_r), buoy displacement (z) and buoy velocity ($\dot{z}$), respectively. Dynamics of the PTO system is not included; nevertheless, its influence on the WEC performance is considered by a constant damping

parameter.

III. PERFORMANCE OF THE WAVE ENERGY CONVERTER

The design of the WEC device defines the performance of the point-absorber system at particular site characterized by a given water depth and wave climate. The size of the floating body determines the hydrostatic parameters of the WEC, which in conjunction with the power take-off system and the device restrictive elements determine the total performance of the WEC. The mathematical model of the WEC dynamics is used to determine its behaviour under different operating conditions [27].

The frequency-dependent hydrostatic parameters of the WEC are obtained by analyzing the structure interactions with the fluid (sea water) using a specialized open-source software named NEMOH, which makes use of the boundary element method (BEM) to compute the first-order wave loads on offshore structures [33]. A comparison between NEMOH and the commercial software WAMIT is carried out in [34], showing a good agreement between them.

For a point absorber system, it is known that a large water plane area of the floating body is related to an increase of its frequency dependent parameters [09] [10]. However, a large diameter might not be practical and its value should be selected properly.

A suitable buoy radius can be selected from the capture width of the point-absorber associated to the maximum theoretical energy extraction defined in (9).

The draft plays an important role on the WEC performance. Unlike the buoy radius, as the draft increases, the excitation force decreases and the radiation damping decreases and tends to zero at lower incident wave frequencies; narrowing the WEC system bandwidth [05] [10] [11] [16]. In addition, a large draft increases the buoy volume; as well as the buoy mass and the system inertia; shifting the natural frequency of the oscillating system towards lower frequencies.

To improve the WEC performance specifically regarding the absorption of wave energy, the geometry of a cylindrical buoy is divided into three sections, which are changed in order to improve the buoy hydrostatic parameters. Several combinations of geometry shapes were evaluated to increase the added mass, whereas the radiation damping was kept as high as possible. As a result, a particular buoy shape is used (see Fig. 1), and its dimensions were evaluated in a parameterization process to tune the natural frequency of the point-absorber WEC system to a frequency within the range of dominant incident waves. A detailed analysis and a description of the buoy geometry sizing process is given in [35].

In the present paper, 25 meters water depth is considered as well as a wave climate characterized by typical wave height of 1 meter and wave periods ranging from 2 to 20 seconds, which covers most of the ocean surface wave characteristics occurring in Mexican coastal waters of the Pacific Ocean [36].

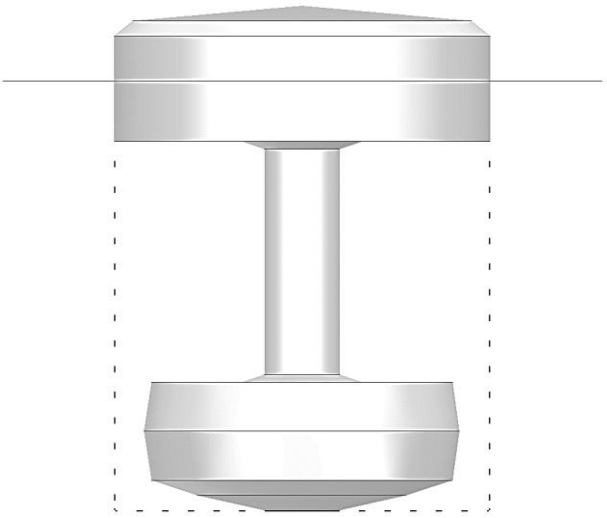

Fig. 1. Buoy structure used in the analysed WEC system; shape obtained from a parametrized process of the buoy geometry to improve its hydrodynamic parameters.

The WEC device that is used consists in a single-body point-absorber that is coupled to a direct-drive PTO placed at the seabed. The PTO system is composed by a linear electric generator; avoiding intermediate elements (gearboxes or similar elements) to convert translational motion into rotary motion, reducing mechanical losses and taking better advantage of the wave energy through the heave motion of the free-water surface.

Generator dynamics is not taken into account, and its influence on the WEC system is represented by a constant damping value that multiplies the velocity of the oscillating system. To evaluate the performance of the WEC, a PTO damping value of 40 $kN \cdot s/m$ (that is obtained by assuming a wave height of 1 meter, a wave period of 4 seconds, a design rated power of 10 kW) and a restoring coefficient of 5 kN/m were used, the later to restrict the buoy displacement.

The upper diameter of the buoy (at free-water surface) is selected as the average value of the capture width associated to wave periods of four and five seconds. That is to say, from (9) is obtained the buoy diameter associated to its maximum theorical power absorption at these wave periods and later, both buoy diameters were averaged, resulting in a buoy diameter of 5 meters. The WEC is tuning to an undamped natural frequency of 1.48 rad/s, corresponding to a wave period of 4.24 seconds; and its performance is analyzed using two buoys: the modified buoy (MB) and a cylindrical buoy (CB) with uniform cross sections (fixed radius) and draft of 3.17 meters, the latter structure is used as a reference.

To obtain the hydrodynamic parameters of the buoy structures, the geometry of the MB is discretized into 4956 nodes and 1829 panels, whereas the CB is discretized into

1180 nodes and 472 panels, the difference in mesh is due the structure shape. The analysis in NEMOH was carried out for 150 angular frequencies in a range from 0.3142 to 3.1416 rad/s, to obtain its frequency dependent parameters. The RAO and the absorbed power are obtained from (6) and (7), respectively.

TABLE I
PHYSICAL BUOY PARAMETERS, WEC SYSTEM TUNED TO AN UNDAMPED NATURAL FREQUENCY OF 1.48 RAD/S.

Buoy	Radius $r_b\ [m]$	Draft $d\ [m]$	Volume $V_b\ [m^3]$	Mass $M_b\ [kg]$
CB	2.5	3.17	62.21	63768.70
MB	2.5	7	42.56	43624.80

The MB has a larger wet surface and lower volume than de CB. At rest, the wet surface of the MB is 90.46 m^2, whereas in the CB is 69.43 m^2. Although the MB has a larger draft than the CB, its hydrostatic parameters are significantly increased, and the radiation damping remains with a larger amplitude for a wider frequency range than the CB (Fig. 2).

A free decay test is performed to show how the buoy damping influences its motion. This test is carried out considering still water and the buoy is hold at 0.5m above the water surface and then it is released. Fig. 3 shows how the motion of the buoy is attenuated along time in absence of incoming waves. It can be seen that the motion of the MB is decreased in less time than CB motion.

The WEC performance in the energy absorption process is carried out in frequency domain. At resonance conditions, where the incident wave frequency is equal to the natural frequency of the WEC, it can be seen that the RAO of the MB reaches a peak amplitude of 1.173 times the wave amplitude and an absorbed power amplitude of 54.707 kW/m^2 (Table II and Fig. 4), whereas the vertical motion of the CB is about 1.028 times the wave amplitude with a maximum power absorption of 40.343 kW/m^2. Moreover, the modified buoy provides a wider frequency bandwidth (Fig. 4) with lower volume and mass as listed in Table I, and Table II shows the WEC absorbed power and the buoy motion in heave at resonant wave frequency.

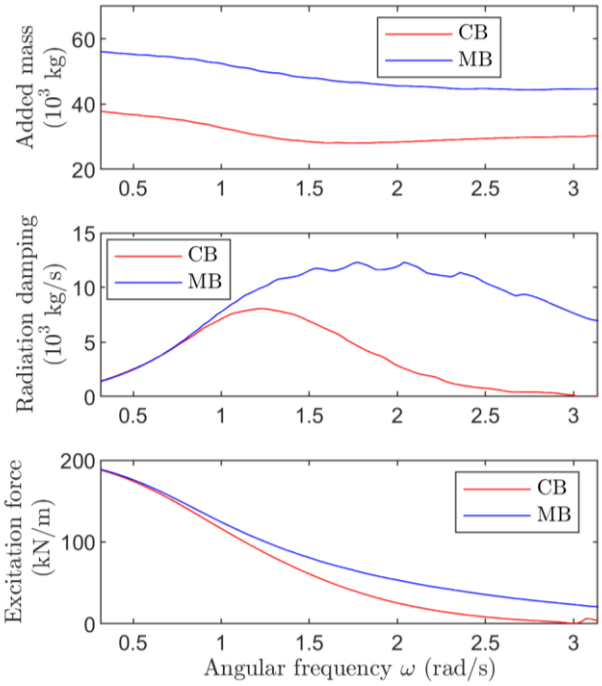

Fig. 2. Hydrodynamic coefficients of the buoy structure obtained from NEMOH. Comparison between a cylindrical buoy (CB) and the composed-structure single-buoy (MB).

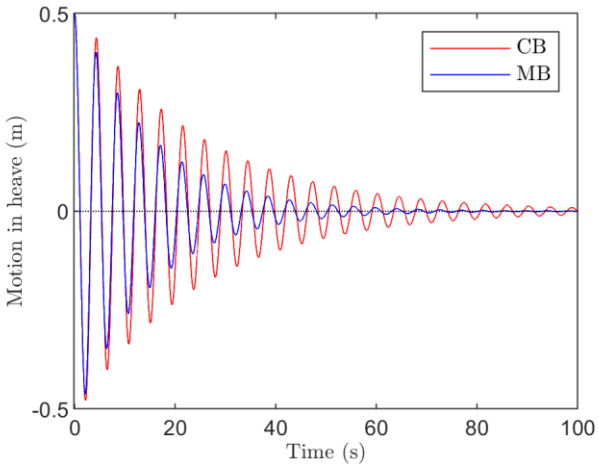

Fig. 3. Free-Decay Test.

TABLE II
WEC PERFORMANCE USING A BUOY WITH CYLINDRICAL SHAPE AND THE PROPOSED SHAPE AT RESONANT WAVE CONDITION.

Buoy	Absorbed power (kW/m²)	RAO peak value
CB	40.343	1.028
MB	54.707	1.173

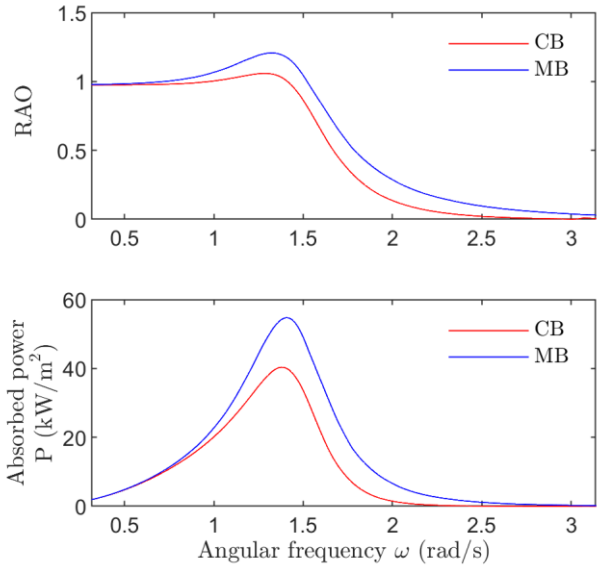

Fig. 4. Point-absorber performance with a constant PTO damping value of 40 kN · s/m. Comparison between a cylindrical buoy (CB) and the modified buoy (MB). (Above) RAO, (Below) Absorbed power.

To confirm the WEC dynamic and performance using the proposed buoy structure, a simulation of the WEC behaviour in the time domain is carried out, comparing its result with the frequency domain. The response of the point absorber device is simulated under a regular incident wave condition, considering a sinusoidal wave with amplitude of 0.5m with an angular frequency of 1.395 rad/s, which is close to the damped natural frequency of both oscillating systems. The PTO system is assumed linear and its dynamics are not considered; however, its influence on the WEC performance is taken into account through a constant damping value of 40 kN · s/m.

Convolution terms related to the radiation and excitation forces are approximated by fourth and sixth order state space subsystems, respectively; and the matrix coefficients are determined by reducing the objective function (15) for the impulse response functions described in (11) and (12). Furthermore, the absorbed power by the PTO system in time domain is calculated at each instant of time using the expression $P_e = B_u \dot{z}^2$.

The state space system that describes the dynamics of the WEC as given by (17), is integrated through a fourth order Runge-Kutta method with a fixed integration step. Assuming that the system is at rest when t = 0, the dynamics of the point absorber system is simulated for a time history of 110 seconds with time intervals of 0.02 seconds to obtain its behaviour in steady state under a regular wave condition.

Figures 5 and 6 show the WEC displacement in heave and its absorbed power, obtained from the point-absorber dynamics in the frequency and time domain for both buoy geometries. For a better appreciation on the waveforms, graphs in the time domain show a time windows of 60 to 90 seconds, which corresponds to a steady state operation of the oscillating system under an excitation source with sinusoidal waveform. In addition, the values of the hydrodynamic performance (average absorbed power (P) and the motion in heave (z)) of the point-absorber device related to the incident wave frequency at incident wave frequency of 1.395 rad/s shown in Table III.

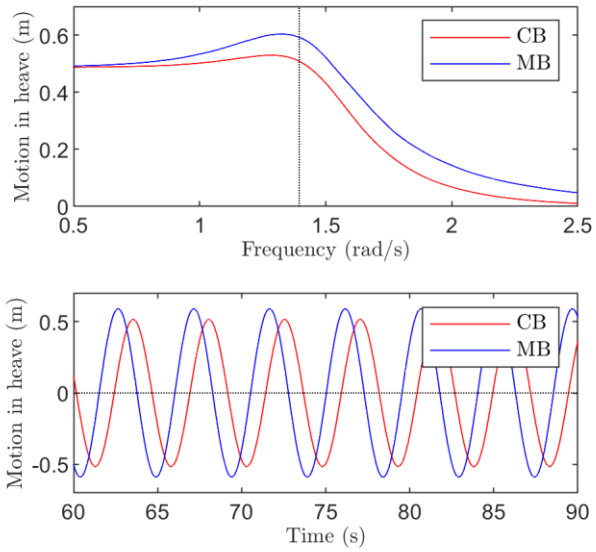

Fig. 5. Buoy displacement at free-water surface under a regular wave condition, incident wave amplitude of 0.5m. (Above) Frequency domain, (Below) Time domain.

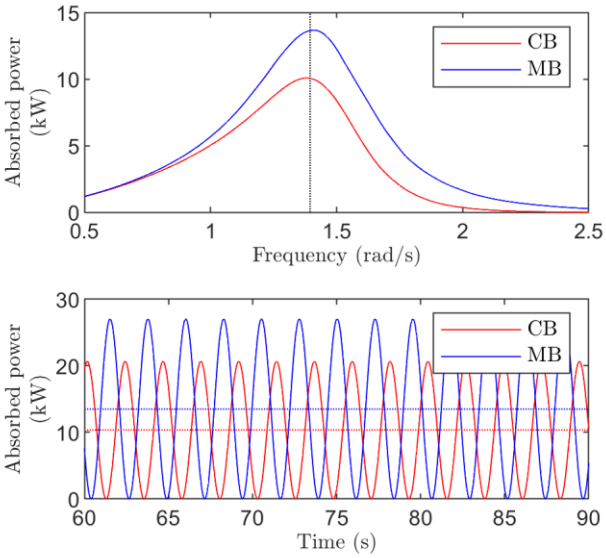

Fig. 6. Absorbed power by the point-absorber WEC under a regular wave condition, incident wave amplitude of 0.5m. (Above) Frequency domain, (Below) Time domain.

TABLE III
WEC PERFORMANCE USING A BUOY WITH CYLINDRICAL SHAPE AND THE MODIFIED SHAPE. USING A REGULAR INCIDENT WAVE WITH AMPLITUDE OF 0.5M AND ω = 1.395 RAD/S (CLOSE TO RESONANT FREQUENCY)

Buoy	Frequency domain		Time domain	
	P [kW]	z [m]	P [kW]	z [m]
CB	10.060	0.5084	10.345	0.5147
MB	13.646	0.5921	13.478	0.5889

Results show a good agreement between the amplitude of the vertical displacement and the average absorbed power of the buoy. Results indicate that using the proposed buoy, the WEC provides a good performance absorbing the wave energy. There is a difference about 1.23 and 0.54 percent in the amplitude of displacement of CB and MB, respectively; whereas for the average absorbed power, the difference is about 2.83 and 1.23 percent, respectively.

An irregular wave profile is obtained from a JONSWAP wave spectrum (defined with a significant wave height of 1 meter, a peak wave frequency of 0.2191 Hz and a peak enhancement factor γ of 1.65) to determine the performance of the WEC device under a relatively realistic operating condition (incident wave with frequency and amplitude varying with time).

As seen in Fig. 7, for an irregular incident wave, the MB provides a better absorption of wave energy than the CB. Therefore, the point-absorber device with the MB could be a suitable option to improve the absorption of wave energy in a point-absorber system placed in waters of finite depth. Moreover, an adequate control scheme could improve the performance of the WEC device, such that, the damping exerted by the PTO system could be tuned to an optimum value depending on the incident wave frequency.

IV. Conclusion

The performance analysis of a point-absorber wave energy converter using a composed buoy structure is carried out to improve its performance at finite depth water for a given sea state. Using a cylindrical buoy with large draft as a reference, a particular buoy geometry is sized, such that the undamped natural frequency of the oscillating system for both buoys is tuned to a given value. Even though the composed-structure buoy has a larger draft than the cylindrical buoy, it has a smaller volume and weight; moreover, the amplitude of the frequency-dependent hydrostatics parameters in the composed single-buoy are increased for a wider frequency range, providing a wider frequency bandwidth than the cylindrical buoy. The dynamics of the PTO system are not considered in the WEC system modelled in time domain.

Comparing the performance of the WEC system for both buoy types indicates that the system with the proposed buoy geometry is able to absorb more energy from incident waves with a wider frequency range, whereas the oscillating system is kept as simple as possible.

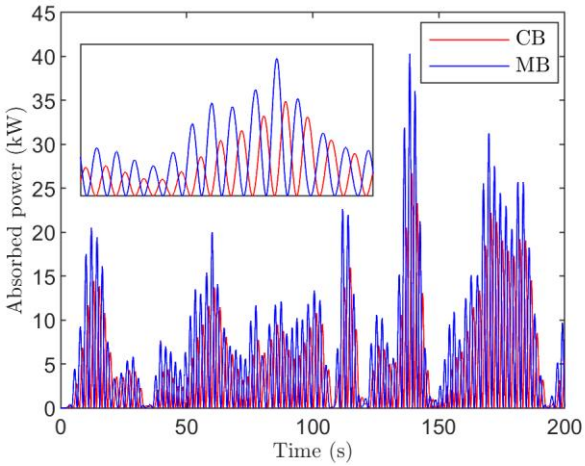

Fig. 7. Estimated absorbed power under irregular wave conditions as results from considering two different buoy structures.

References

[01] Johannes Falnes, "A review of wave-energy extraction", *Marine Structures*, vol. 20, pp. 185–201, 2007 DOI: doi.org/10.1016/j.marstruc.2007.09.001

[02] J. Faiz, M. Ebrahimi-Salari, "Comparison of the Performance of Two Direct Wave Energy Conversion Systems: Archimedes Wave Swing and Power Buoy", *Journal of Marine Science and Application*, vol. 10, pp. 419-428, 2011, DOI: 10.1007/s11804-011-1087-9

[03] A. F. de O. Falcão, "Wave energy utilization: A review of the technologies", *Renewable and Sustainable Energy Reviews*, vol. 14, pp. 899–918, 2010, DOI: doi.org/10.1016/j.rser.2009.11.003

[04] M. E. McCormick, "Ocean wave energy concepts", *OCEANS '79*, pp. 553-558, 1979, DOI: doi.org/10.1109/OCEANS.1979.1151266

[05] J. Falnes and J. Hals, "Heaving buoys, point absorbers and arrays", *Philosophical Transactions of The Royal Society A: Mathematical, Physical and Engineering Sciences*, vol. 370, pp. 246–277, 2011, DOI: doi.org/10.1098/rsta.2011.0249

[06] J. Falnes, "Optimum control of oscillation of wave-energy converters, in Annex Report B1: Device Fundamentals/Hydrodynamics of the Wave Energy Converters: Generic Technical Evaluation Study", Commission of the European Communities, 1993

[07] M. Greenhow, S. P. White, "Optimal heave motion of some axisymmetric wave energy devices in sinusoidal waves", *Applied Ocean Research*, vol. 19, pp. 141-159, 1997, DOI: doi.org/10.1016/S0141-1187(97)00020-5

[08] W. Sheng, R. Alcorn, and A. Lewis, "On improving wave energy conversion, part II: Development of latching control technologies", *Renewable Energy*, vol. 75, pp. 935-944, 2015, doi:10.1016/j.renene.2014.09.049

[09] M. Eriksson, J. Isberg, and M. Leijon, "Hydrodynamic modelling of a direct-drive wave energy converter", *International Journal of Engineering Science*, vol. 43, pp. 1377–1387, 2005, DOI: doi.org/10.1016/j.ijengsci.2005.05.014

[10] L. Sjökvist, R. Krishna, M. Rahm, V. Castellucci, A. Hagnestål and M. Leijon, "On the Optimization of Point Absorber Buoys", *Journal of marine science and engineering*, vol. 2, pp. 477-492, 2014, DOI: doi.org/10.3390/jmse2020477

[11] M. A. Stelzer and R. P. Joshi, "Evaluation of wave energy generation from buoy heave response based on linear generator concepts", *Journal of Renewable and Sustainable Energy*, vol. 4, 063137, 2012, DOI: doi.org/10.1063/1.4771693

[12] T. Usha, "Power absorption by thin wave devices", *Applied Mathematical Modelling*, vol. 14, pp. 327-333, 1990, DOI: doi.org/10.1016/0307-904X(90)90085-J

[13] H. Sarlak, M. S. Seif, and M. Abbaspour, "Experimental Investigation of offshore wave buoy performance", *Journal of Marine Engineering*, vol. 6, pp. 1-11, 2010

[14] S. Jin, R. Patton, "Geometry Influence on Hydrodynamic Response of a Heaving Point Absorber Wave Energy Converter", *12th European Wave and Tidal Energy Conference (EWTEC)*, 2017

[15] Z. Wan-chao, L. Heng-xu, Z. Liang, Z. Xue-wei, "Hydrodynamic analysis and shape optimization for vertical axis-symmetric wave energy converters", *China Ocean Eng.*, vol. 30, pp. 954-966, 2016, DOI: 10.1007/s13344-016-0062-2

[16] G. De Backer, "Hydrodynamic Design Optimization of Wave Energy Converters Consisting of Heaving Point Absorbers", Doctoral dissertation, Ghent University, 2009

[17] J. Pastor and Y. Liu, "Frequency and time domain modeling and power output for a heaving point absorber wave energy converter", *International Journal of Energy and Environmental Engineering*, vol. 5, 101, 2014, DOI: doi.org/10.1007/s40095-014-0101-9

[18] M. Vantorre, R. Banasiak, and R. Verhoeven, "Modelling of hydraulic performance and wave energy extraction by a point absorber in heave", *Applied ocean research*, vol. 26, pp. 61-72, 2004, DOI: doi.org/10.1016/j.apor.2004.08.002

[19] A. Josefsson, A. Berghuvud, K. Ahlin, and G. Broman, "Performance of a Wave Energy Converter with Mechanical Energy Smoothing", *European Wave and Tidal Energy Conference (EWTEC)*, 2011

[20] A. H. Sakr, Y. H. Anis, and S. M. Metwalli, "System frequency tuning for heaving buoy wave energy converters", *IEEE International Conference on Advanced Intelligent Mechatronics*, pp. 1367-1372, 2015, DOI: doi.org/10.1109/AIM.2015.7222729

[21] S. Olaya, B. Jean-Matthieu, M. Benbouzid, "Modelling and Preliminary Studies for a Self-Reacting Point Absorber WEC", *First International Conference on Green Energy (ICGE)*, 2014, DOI: https://doi.org/10.1109/ICGE.2014.6835390

[22] L. Berggren and M. Johansson, "Hydrodynamic coefficients of a wave energy device consisting of a buoy and a submerged plate", *Applied Ocean Research*, vol. 14, pp. 51-58, 1992, Elsevier. DOI: https://doi.org/10.1016/0141-1187(92)90007-7

[23] M. Blanco, M. Lafoz, and G. Navarro, "Wave energy converter dimensioning constrained by location, power take-off and control strategy", *IEEE International Symposium on Industrial Electronics*, pp. 1462-1467, 2012, DOI: doi.org/10.1109/ISIE.2012.6237307

[24] J. Engström, V. Kurupath, J. Isberg, and M. Leijon, "A resonant two-body system for a point absorbing wave energy converter with direct-driven linear generator", *Journal of applied physics*, vol. 110, 124904, 2011, DOI: doi.org/10.1063/1.3664855

[25] J. Engström, M. Eriksson, J. Isberg, and M. Leijon, "Wave energy converter with enhanced amplitude response at frequencies coinciding with Swedish west coast sea states by use of a supplementary submerged body", *Journal of applied physics*, vol. 106, 064512, 2009, DOI: doi.org/10.1063/1.3233656

[26] M. McCormick, Ocean engineering mechanics with applications, Cambridge University Press, 2009

[27] J. Cruz, Ocean Wave Energy: Current Status and Future Perspectives, Springer, 2007

[28] J. Falnes, Ocean waves and oscillating systems: linear interactions including wave-energy extraction, Cambridge University Press, 2002

[29] W. E. Cummins, "The impulse response function and ship motions", Report 1161, October 1962

[30] Z. Yu and J. Falnes, "State-space modelling of a vertical cylinder in Heave", *Applied Ocean Research*, Elsevier, vol. 17 pp. 265-215. Dec. 1995, DOI: https://doi.org/10.1016/0141-1187(96)00002-8

[31] Z. Yu and J. Falnes, "State-space modelling of dynamic system in ocean engineering", *Journal of hydrodynamics*, Ser. B, pp. 1-17, 1998

[32] J. Falnes, "On non-causal impulse response functions related to propagating water waves", *Applied ocean research*, vol. 17, pp. 379-389, 1995, https://doi.org/10.1016/S0141-1187(96)00007-7

[33] A. Babarit, and G. Delhommeau, "Theoretical and numerical aspects of the open source BEM solver NEMOH", *11th European Wave and Tidal Energy Conference (EWTEC)*, 2015

[34] A. Roessling and J. Ringwood, "Finite order approximations to radiation forces for wave energy applications", *Renewable Energies Offshore*, CRC Press, pp. 359-366, 2015

[35] A. Ruezga, J. M. Cañedo, "Buoy Analysis in a Point-Absorber Wave Energy Converter", *IEEE Journal of Oceanic Engineering*, 2019, DOI: doi.org/10.1109/JOE.2018.2889529

[36] A. I. Pérez Peña, "Estimación del clima marítimo y la energía del oleaje disponible en las costas mexicanas", Master's thesis, Universidad Nacional Autónoma de México, 2012.